Jurnal Ilmiah Teknik Elektro Komputer dan Informatika (JITEKI)
Vol. 8, No. 3, September 2022, pp. 422-430
ISSN: 2338-3070, DOI: 10.26555/jiteki.v8i3.23636

Classification of Gender Individual Identification Using Local Binary Pattern on Palatine Rugae Image

Hilman Fauzi [1], Cynthia Erika [2], Sofia Sa'idah [3], Fahmi Oscandar [4]
[1,2,3] Faculty of Electrical Engineering, Telkom University, Bandung, Indonesia
[4] faculty of Dentistry, Universitas Padjajaran, Bandung, Indonesia

ARTICLE INFO

Article history:

Received March 20, 2022
Revised May 31, 2022
Accepted October 27, 2021

Keywords:

Gender;
Identification;
K Nearest Neighbor;
Local Binary Pattern;
Palatine Rugae

ABSTRACT

Major disasters caused many casualties with the condition of the damaged bodies. It causes the individual identification process to be ineffective through biometric characteristics (such as lips and fingerprints). However, the palatine rugae can carry the individual identification process. Palatine rugae have unique and individual characteristics and are more resistant to trauma because of their internal location. In this study, an individual identification system is proposed to identify gender using the image of palatine rugae. The proposed system is developed by several algorithms and methods, such as Local Binary Pattern (LBP) as the feature extraction method and K-Nearest Neighbor (KNN) as the classification method. Based on the result of the system performed test, the proposed system can identify the gender of an individual by the combination of recognized palatine rugae patterns. The system achieved an accuracy test result of 100% with a specific configuration of LBP and KNN. The research contribution in this study is to develop the individual gender identification system, which proceeds with the palatine rugae pattern image with unique biometric characteristics as an input. The system applied several methods and algorithms, such as Geometric Active Contour (GAC) as a segmentation algorithm, Local Binary Pattern (LBP) as a feature extraction method, and K Nearest Neighbor (KNN) as a classification method.

Hilman Fauzi,
Biomedical Engineering, Faculty of Electrical Engineering, Telkom University, Indonesia
Email: hilmanfauzitsp@telkomuniversity.ac.id

1. INTRODUCTION

Indonesia is a country that is prone to natural disasters. Natural disasters that occur massively cause significant damage to the victim's body. The missing or damaged body parts make the deceased victims unable to be appropriately identified. In these circumstances, the application of victim identification by the lip, fingerprint, tooth, or bone method cannot be used because it is ineffective. These limitations have made it difficult for forensic odontologists to identify victims. Forensic odontology is a branch of medical science that helps investigators determine individual identities in mass disasters. The point of legal odontology is to assess the demonstrative quality of the autopsy odontogram carried out remotely through a video of the verbal depth utilizing an intra-oral camera. Exceptionally few consider having inquired about teledentistry within the field of forensic dentistry. The scientific dental specialist, a part of the legal team, is commissioned, for the case, by the legal specialists to identify cadavers and ponder chomp marks on living or expired persons.

Several studies have been conducted on individual identification methods; one is palatine rugae. Palatine rugae are unpredicTable transverse edges of the mucosa in the front third of the sense of taste, emanating from the palatine raphae behind the sharp papillae [1]. Palatine rugae are permanent and unique to each person [2]. A cross-sectional think of 239 Korean children who matured under 13 long time ancient and 61 adolescents who matured 13 long times and older illustrated that the number of palatine rugae a childhood or youth was comparative [3]. In another study, it can be concluded that all rugae appeared to have positional

changes, increased lengths, and lower numbers but no noteworthy shape changes with development. The lengths, numbers, and positions of the rugae were influenced by orthodontic treatment, particularly their sidelong focuses, but the personal characteristics of the palatine rugae did not alter [4]. In addition, age, race, and genders also affect the number of patterns found in rugae. The palatine rugae within the Lebanese population show shape distinct from other detailed Mediterranean and non-Caucasian populaces. According to Asmaa Fady Sherif et al., the curve pattern is more significant in Malaysian men than in Egyptian men. In contrast, the wavy pattern in Malaysian women is more significant than in Egyptian women. They are a sTable landmark, the palatine rugae also can play a significant role in clinical dentistry, so they can be used as an option to assist the identification process [5]. Palatine rugae are found to be steady in shape and structure during the life of a person and are not changed by disease, trauma, chemicals, or heat [6][7][8]. Once shaped, they stay in the same position and, indeed, in case they are devastated, are reproduced precisely at their unique site [6][8]. Their soundness is due to their anatomical position interior the verbal depression, which protects them by the lips, cheeks, tongue, teeth, and bone and prosthetic gadgets. Moreover, they resist thermal effects in burn victims and decay changes for up to seven days after death [9][10]. Besides, palatine rugae can identify edentulous subjects when other odontological methods cannot be used [11]. Numerous endeavors have been made in this field to record and examine information to create a reliable and straightforward way for personal identification [12].

The research contribution in this study is to develop the individual gender identification system, which proceeds with the palatine rugae pattern image with unique biometric characteristics as an input. The system applied several methods and algorithms, such as Geometric Active Contour (GAC) as a segmentation algorithm, Local Binary Pattern (LBP) as a feature extraction method, and K Nearest Neighbor (KNN) as a classification method.

2. METHOD

The research method is shown in Fig. 1. It will be explained in the next section.

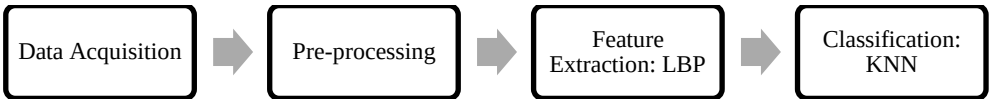

Fig. 1. Proposed method for palatine rugae classification

2.1. Data Acquisition

Data or image acquisition is the step of collecting data that will be used for defined the data pattern for system testing purposes. This study develops the gender identification system with 200 palatine rugae images as data input. The used images are a print of the palatine rugae that have been marked on the outline of the palatine rugae pattern using a marker. The outlined palatine rugae pattern image print is then photographed and saved in .jpg format. The sample data of the palatine rugae image is shown in Fig. 2.

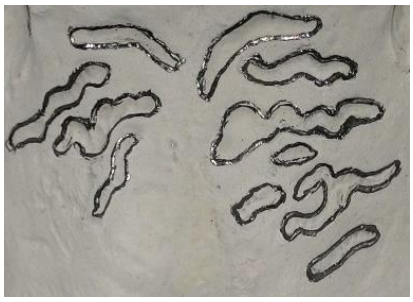

Fig. 2. Sample of Data Study

2.2. Pattern Identification

The rugae design was recorded agreeing to Gayathri [13] as wavy, bent, straight, and circular concurring with Chopra et al. [14] as unification/branching assist classified as separating or converging depending on the sort of beginning. Any other frame which did not fit into the criteria was classified as non-specific. The pattern classification used in this study refers to the classification of palatine rugae based on Thomas and Kotze. Patterns will be divided into five types: unification, wavy, curved, straight, and circular. The shape of each pattern can be seen in the image Fig. 3 [13]. The palatine rugae patterns are shown in Fig. 3.

Fig. 3. Type of palatine rugae pattern. Name of palatine rugae pattern: 1- straight; 2- circular; 3- curved; 4- wavy; 5- divergent; 6- convergent.

Thomas and Kotze classification were utilized to interpret palatine rugae on the casts. The rugae were sketched out with a sharp pencil and measured using a computerized Vernier Caliper [15]. The rugae are classified based on their length as the following: primary (>5 mm), secondary (3–5 mm), and fragmentary (<3 mm). Rugae less than 3 mm are neglected. The rugae are separated into four shapes: shape unification, curve, wavy, straight, and circular [16]. This study used Thomas and Kotze's classification standard to differentiate the gender based on the palatine rugae pattern. Thomas and Kotze said that there were differences in the dominance of the appearance of the pattern in the male and female palatine rugae. Males are dominated by wavy, straight, curved patterns and unified, circular patterns. In women, the more dominant patterns are wavy and curved patterns, followed by straight patterns and unification.

2.3. Pre-Processing

Pre-processing is the preparation stage to improve efficiency and image quality used for the feature extraction process. The process is divided into five steps: RGB to grayscale conversion, Filtering Gaussian, grayscale to BW image conversion, and Morphologic process: dilation, Cropping, and segmentation ROI.

2.4. RGB to Grayscale

The input image with the primary colors green, red, and blue; needs to be changed to gray. The gray image has only one intensity value for each pixel, ranging from 0 to 255 [17][18]. The difference between RGB and grayscale images can be seen in Fig. 4.

(a) (b)

Fig. 4. RGB and Grayscale Image (a) RGB Image (b) Grayscale image

2.5. Gaussian filters

After being converted into a gray image, the image will be refined using a Gaussian filter to remove noise to increase the detail in the image. The Gaussian filter makes the image smoother by normalizing the extreme value pixel [19]. The image of the Gaussian filter can be seen in Fig. 5.

2.6. BW Image

This process converts the palatine rugae image into BW or binary image. This BW image conversion process aims to facilitate the morphological pattern process at the next step. The BW image is illustrated in Fig. 6.

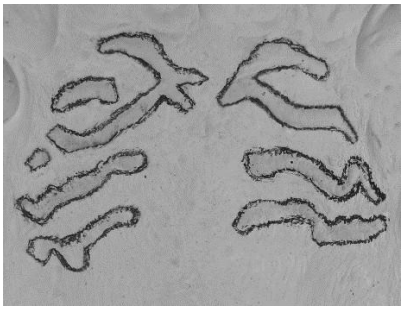

Fig. 5 Gaussian Filtered Image

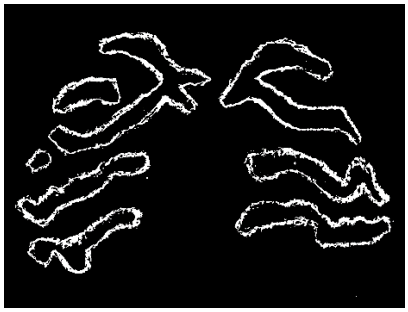

Fig. 6. BW Image

2.7. Dilation

A dilation is a form of image morphology, which is adding pixels to object boundaries or restoring damaged (lost) image shapes in binary images [20][21]. In this study, morphology is used to determine the structure of the palatine rugae pattern. The dilated image is illustrated in Fig. 7.

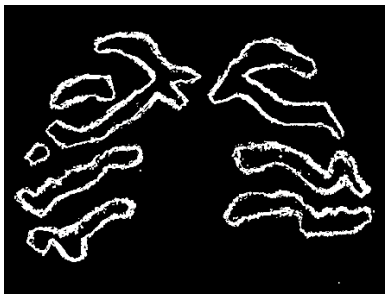

Fig. 7. Dilated Image

2.8. Region of Interest (ROI)

The ROI cropping or segmentation is carried out to get the specific area in the pattern part of the palatine rugae image. The feature extraction process facilitates the calculation and analysis process in pattern recognition. In this study, Geometric Active Contour (GAC) method is used as the image segmentation method [22][23]. In the segmentation process, thresholding is performed based on the image's differences in gray levels [24], [25]. Segmentation was carried out by separating the pattern of palatine rugae with a rectangular frame. GAC is one of the segmentation methods that Kass first introduced. The inadequacy of dynamic geometric forms is that they are amazingly delicate to initialization positions. The show is inclined to fall into false boundaries, spilling from the soft edge and destitute anti-noise ability.

Consequently, active forms can extend or shrivel from initialization, making strides the impediments of destitute vigor to initialization and unidirectional development [26]. The forms of the objects are initialized and advanced at the same time within the given pictures. As the forms continue towards the boundary of the common object(s) displayed within the pictures, vitality esteem gets decreases. The forms are permitted to advance until both the internal and the external forms coincide at the protest boundary [27]. This method is influenced by energy which is written by the equation as [28][29]:

$$E_{snake} = \int_0^1 \{E_{int}(v(s)) + E_{img}(v(s)) + E_{con}(v(s))\} ds \quad (1)$$

Where E_{snake} is an active contour energy function. E_{int} is the internal energy of the active contour, which is influenced by the curve and movement of the object. E_{img} is the energy of the digital image that is entered. E_{con} will draw the contour to widen or narrow towards the desired object. The image of the palatine rugae pattern resulting from the cropping and segmentation process can be seen in Fig. 8.

2.9. Local Binary Pattern (LBP)

This process is performed to get the particular characteristics of palatine rugae pattern images. The different pattern characteristics of palatine rugae images will be identified in a unique mathematical pattern. The segmented palatine rugae image features are extracted using LBP parameters such as P and R. P is the number of adjacent pixels, and R is the radius between the center and adjacent pixels. In the LBP calculation

process, a threshold value is needed to be defined: the value of the middle pixel in a block of pixels [30][31]. Then, the pixel value will be compared with the adjacent pixel value. Once the middle value is defined, the other pixel values are compared. If the adjacent pixel value is lower than the threshold value, the pixel is assigned a binary value of 0. However, if the neighboring pixel value is higher than or equal to the neighboring pixel value, the pixel will be assigned a binary value of 1 [32]. After obtaining 8 bits of a binary value, the bit values are sorted following a clockwise pattern starting from row one and column one so that a binary series is arranged [33]. After the binary series are formed, the binary patterns are mapped by multiplying the binary values according to their weight values in their respective positions. The mapped binary pattern results are added to replace the middle pixel value. The binary value that has been obtained from the LBP method will be converted back into the form of a decimal value. Then the input image will be resized according to the specified dimensions. In this study, the resolution of the input image is 320×240.

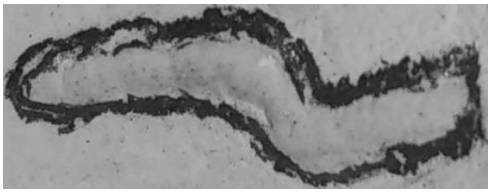

Fig. 8. The Image of Palatine Rugae Pattern Result of Cropping and Segmentation

2.10. K Nearest Neighbor

KNN classifies the features of palatine rugae images based on the combination of patterns that have been recognized before. The output images of five rugae pattern types will be obtained and used as features in gender identification. Classification is needed to facilitate finding similar patterns in the very diverse images of palatine rugae. The KNN classification proceeds using four distance calculations: euclidean, cosine, city block, and correlation [34][35]. In addition, to determine the effect of the K value on the classification process, KNN is conFig.d using K values of 1, 3, 5, 7, and 9. In determining the proximity or metric distance from the center to the nearest sample in the KNN method, several formulas can be used, including:

a. Euclidean Distance

In calculating the distance between two points, it can be found by the following equation [26][27][36][37] [38]:

$$Dxy = \sqrt{\sum_{i=1}^{n} (x_i - y_i)^2} \tag{2}$$

Where D is the proximity distance, x is the training data, y is the testing data, i is the individual attribute with values 1 to n, and n is the number of individual attributes.

b. Cosine Distance

In this calculation, the cosine distance is calculated by one minus the cos value of the angle between two points defined as follows [10][37][39][38]:

$$d_{s,t} = 1 - cos\,\theta \tag{3}$$

where,

$$\cos\theta = \frac{XsXt}{|Xs||Xt|} \tag{4}$$

c. City Block Distance

City Block Distance calculates the distance between two points from the total difference in the absolute value of the Cartesian coordinates written with the following equation [7][27][36][40]:

$$d_{s,t} = \sum_{j-1}^{n} |s_j - t_j| \tag{5}$$

d. Correlation Distance

In correlation distance, the points are considered as a series of values. The distance between the values of x_s and x_t can be calculated by the following equation [10] [1][36]:

$$d_{s,t} = (1 - \frac{(x_s - \bar{x_s})(x_t - \bar{x_t})}{((x_s - \bar{x_s})(x_s - \bar{x_s}), (x_t - \bar{x_t})(x_t - \bar{x_t})}) \quad (6)$$

with s, t is the coordinates of the object point, and n is the number of objects.

3. RESULT AND DISCUSSION

System performance testing is calculated in accuracy and computation time involving four parameters. Those parameters are kernel size and radius (R) on LBP as feature extraction, K value, and distance calculation method on KNN as classification method on the system.

3.1. Effect of Kernel Size

The test was conducted to determine the effect of the system on the kernel size. The system is tested using kernel sizes of 2×2, 3×3, 4×4, and 5×5. Based on the test results, it was found that the highest accuracy occurred in 2×2 and 4×4 of kernel sizes with 83%. However, system performance with a 4×4 kernel size is considered better because of the 6.4% shorter computation time of 1.31 seconds. The system showed higher performance in odd kernel sizes (3×3 and 5×5) compared to even kernel sizes (2×2 and 4×4) with 17% and 67% accuracy. Kernel size with odd values can optimize the calculation of the image matrix in the feature extraction process in LBP. The results of system testing on kernel size can be seen in Table 1.

Table 1. Kernel size test results

Kernel Size	Accuracy	Computation Time (s)
2×2	83%	1.56
3×3	17%	1.39
4×4	83%	1.46
5×5	67%	1.31

3.2. The Effect of R

The purpose of the test is to determine the effect of radius size (R) on the accuracy and computational time of the system. The tests were carried out on the sizes of Radius 1, 2, and 3. Based on the test results, the best system performance occurred with R=3 with an accuracy of 83% and a computation time of 61.7 seconds. In addition, the system performance showed a better performance in accuracy and computation time linearly with the increment of R size. Increasingly widespread R size, the area used as a reference for comparison is also wider. Thus, the required time to proceed with the pixels to be characterized will be less. The results of R size testing on the system can be seen in detail in Table 2.

Table 2. R-value test results

R Size	Accuracy	Computation Time (s)
1	50%	71.7
2	50%	63.79
3	83%	61.7

3.2. Effect of K value and Distance Calculation Type

The test is conducted to determine the effect of the K value and the type of distance calculation on the KNN on system performance by measuring the accuracy and computational time of the system. Based on the test results, on average, the highest accuracy occurs in the cosine distance type with a value of 67%. While the highest average of accuracy based on the value of K occurs at K = 3 with an accuracy of 67%. However, the highest accuracy with a combination of K values and the type of distance calculation is achieved in K=7 and cosine distance calculation method with an accuracy of 100%. The detailed accuracy calculation results can be seen in Table 3.

In another case, the average time required to process data is 0.1 seconds in calculating the system's computational time. The difference in computation time for each type of distance calculation and the value of K is minimal on the order of 10-3, so it is not significant enough to affect overall system performance. Thus, regardless of the value of K and the distance calculation method of KNN, the resulting computational time is relatively the same at 0.1 seconds. The results of calculating system computing time based on different distance calculations and K values can be seen in Table 4.

Table 3. KNN Type Accuracy Results with Different K Values and Distance Method

Distance method	Accuracy (%)					Average (%)
	1	3	5	7	9	
Cosine	50	83	67	100	33	**67**
City Block	50	50	50	33	33	**43**
Euclidean	33	83	83	33	17	**50**
Correlation	33	50	33	50	17	**37**
Average	**42**	**67**	**58**	**54**	**25**	

Table 4. Results of Computing Time for Types of KNN with Different K Values

Distance method	Computation Time (s)					Average
	1	3	5	7	9	
Cosine	0.097	0.109	0.108	0.101	0.121	**0.107**
City Block	0.111	0.102	0.110	0.110	0.125	**0.112**
Euclidean	0.114	0.111	0.101	0.105	0.078	**0.102**
Correlation	0.101	0.102	0.105	0.103	0.103	**0.103**
Average	**0.106**	**0.106**	**0.106**	**0.105**	**0.107**	

4. CONCLUSION

Based on the results of three types of system testing, it can be concluded that the palatine rugae pattern image processing can identify an individual gender. The gender identification system is performed optimally with the configuration of LBP as a feature extraction method and KNN as a classification method by selecting the best parameters. In detail, the proposed system was compiled optimally with the 4×4 kernel and the value of R=3 on the LBP. On the KNN configuration, the proposed system is optimally compiled by the distance calculation method of cosine with K=7. Finally, this study has proven that an individual gender can be identified through image processing of palatine rugae with excellent accuracy and performance. Therefore, it has raised the opportunities for further study of forensic technology.

REFERENCES

[1] M. Jog, A. Pandey, and M. S. Dahiya, "The Role of Ante-Mortem Records of Palatal Rugae in Disaster Victim Identification (DVI)," *International Journal of Scientific Research in Science and Technology*, vol. 2, no. 6, pp. 395–400, 2016, https://ijsrst.com/IJSRST162630.

[2] R. S. Basman, R. T. Achmad, D. R. Utari, T. Rona, A. Harya, and E. I. Auerkari, "Types of Palatal Rugae for Sex Determination in the Indonesian Subpopulation," *Journal of International Dental and Medical Research*, vol. 12, no. 4, pp. 1433-1435, http://www.jidmr.com/journal/wp-content/uploads/2019/12/32.14238.pdf.

[3] N.-H. Kim, Y.-G. Im, J.-Y. Kim, and B.-G. Kim, "Palatal Rugae Pattern in Korean Children and Adolescents," *J Oral Med Pain*, vol. 44, no. 4, pp. 169–173, 2019, https://doi.org/10.14476/jomp.2019.44.4.169.

[4] J. A. Chong, A. M. F. S. Mohamed, and A. Pau, "Morphological patterns of the palatal rugae: A review," *J Oral Biosci*, vol. 62, no. 3, pp. 249–259, 2020, https://doi.org/10.1016/j.job.2020.06.003.

[5] A. F. Sherif, A. A. Hashim, M. A. al Hanafy, and E. M. Soliman, "A pilot- cross sectional study of palatal Rugae shape and direction among Egyptians and Malaysians," *Egypt J Forensic Sci*, vol. 8, no. 1, pp. 1–9, 2018, https://doi.org/10.1186/s41935-018-0050-1.

[6] V. Hermosilla Venegas, J. San Pedro Valenzuela, M. Cantín López, and I. C. Suazo Galdames, "Palatal Rugae: Systematic Analysis of its Shape and Dimensions for Use in Human Identification," *International Journal of Morphology*, vol. 27, no. 3, pp. 819–825, 2009, https://doi.org/10.4067/S0717-95022009000300029.

[7] R. Kamala, N. Gupta, A. Bansal, and A. Sinha, "Palatal rugae pattern as an aid for personal identification: a forensic study," *Journal of Indian Academy of Oral Medicine and Radiology*, vol. 23, no. 3, pp. 173-178, 2011, https://www.proquest.com/docview/926228703?pq-origsite=gscholar&fromopenview=true.

[8] S. S. M., K. Shalini, and A. Akshari, "Cheloscopy-a Unique Forensic Tool," *Journal of Health and Allied Sciences NU*, vol. 03, no. 04, pp. 074–077, 2013, https://doi.org/10.1055/s-0040-1703706.

[9] G. de A. A. Rosa *et al.*, "Computerized morphometry of the area of the hard palate and of palatal rugae: a cross-sectional study," *Medicina Legal de Costa Rica*, vol. 37, no. 1, pp. 154–161, 2020.https://www.scielo.sa.cr/scielo.php?pid=S1409-00152020000100154&script=sci_arttext.

[10] M. A. Nur, N. Djustiana, and Y. Malinda, "Description of palatal rugae size and direction in children with gender difference," *Padjadjaran Journal of Dentistry*, vol. 30, no. 1, p. 41, 2018, https://doi.org/10.24198/pjd.vol30no1.14323.

[11] R. Almasudi, G. Somashekarachar, N. Doggalli, M. S. Iyer, S. Srinivas, and A. Aradhya, "Evaluation and Comparison of Different Palatal Rugae Patterns between Dentulous and Edentulous Population of Mysuru City – A Preliminary Forensic Survey," *J. Evol. Med. Dent. Sci.*, vol. 10, no. 25, pp. 1910–1916, 2021, https://doi.org/10.14260/jemds/2021/394.

[12] S. K. V. S. Renu Kumari, "Study of Palatal Rugae for Forensic Identification," *International Research Journal of Engineering and Technology (IRJET)*, vol. 8, no. 4, pp. 3272–3274, 2021.

https://www.irte.com/researches/Research%20Paper%20Renu%20Sujit%20Vishal.pdf.
[13] M. Gayathri and A. C. Kanthasawmy, "Comparing the potential role of palatal rugae pattern in paternal testing-A cross sectional study," *Indian Journal of Forensic Medicine and Toxicology*, vol. 13, no. 2, pp. 61–67, 2019, https://doi.org/10.5958/0973-9130.2019.00086.0.
[14] S. Chopra, P. Bansal, and P. Bansal, "Essix Appliance- An Innovation Modification for use as Temporary Bridge-A Case Report," *J Adv Med Dent Scie Res*, vol. 8, no. 1, pp. 184–186, 2020, http://jamdsr.com/uploadfiles/44ESSIXAPPLIANCEVOL8ISSUE1PP184-186.20200221072919.pdf.
[15] M. Bisht, P. Rawat, R. Madan, and S. Tripathi, "Anthropometric analysis of palatal rugae pattern, face form and arch form among Indian population at Moradabad, India," *International Dental Journal of Student's Research*, vol. 6, no. 1, pp. 13–17, 2020, https://doi.org/10.18231/2278-3784.2018.0003.
[16] A. R. Malekzadeh, H. R. Pakshir, S. Ajami, and F. Pakshir, "The application of palatal rugae for sex discrimination in forensic medicine in a selected Iranian population," *Iran J Med Sci*, vol. 43, no. 6, pp. 612–622, 2018, https://www.ncbi.nlm.nih.gov/pmc/articles/PMC6230942/.
[17] G. K. Ijemaru, et al., "Image processing system using MATLAB-based analytics," *Bulletin of Electrical Engineering and Informatics*, vol. 10, no. 5, pp. 2566-2577, https://doi.org/10.11591/eei.v10i5.3160.
[18] T. Kumar and K. Verma, "A Theory Based on Conversion of RGB image to Gray image A Theory Based on Conversion of RGB image to Gray image," no. April 2016, pp. 6–10, 2010, https://doi.org/10.5120/1140-1493.
[19] O. L. Usman, R. C. Muniyandi, K. Omar, and M. Mohamad, "Gaussian smoothing and modified histogram normalization methods to improve neural-biomarker interpretations for dyslexia classification mechanism," *PLoS One*, vol. 16, no. 2, 2021, https://doi.org/10.1371/journal.pone.0245579.
[20] A. M. Raid, W. M. Khedr, M. A. El-dosuky, and M. Aoud, "Image Restoration Based on Morphological Operations," *International Journal of Computer Science, Engineering and Information Technology*, vol. 4, no. 3, pp. 9–21, 2014, https://doi.org/10.5121/ijcseit.2014.4302.
[21] K. A. M. Said and A. B. Jambek, "Analysis of Image Processing Using Morphological Erosion and Dilation," *J Phys Conf Ser*, vol. 2071, no. 1, 2021, https://doi.org/10.1088/1742-6596/2071/1/012033.
[22] J. Ma, D. Wang, X.-P. Wang, and X. Yang, "A Characteristic Function-Based Algorithm for Geodesic Active Contours," *SIAM J Imaging Sci*, vol. 14, no. 3, pp. 1184–1205, 2021, https://doi.org/10.1137/20M1382817.
[23] L. Sun, X. Meng, J. Xu, and Y. Tian, "An image segmentation method using an active contour model based on improved SPF and LIF," *Applied Sciences*, vol. 8, no. 12, pp. 1–20, 2018, https://doi.org/10.3390/app8122576.
[24] R. V. Nahari, A. Jauhari, R. Hidayat, and R. Alfita, "Image Segmentation of Cows using Thresholding and K-Means Method," *International Journal of Advanced Engineering, Management and Science*, vol. 3, no. 9, pp. 913–918, 2017, https://dx.doi.org/10.24001/ijaems.3.9.2.
[25] N. Kulkarni, "Color Thresholding Method for Image Segmentation of Natural Images," *International Journal of Image, Graphics and Signal Processing*, vol. 4, no. 1, pp. 28–34, 2012, https://doi.org/10.24001/ijaems.3.9.2.
[26] A. Ghosh and S. Bandyopadhyay, "Image co-segmentation using dual active contours," *Applied Soft Computing Journal*, vol. 66, pp. 413–427, 2018, https://doi.org/10.1016/j.asoc.2018.02.034.
[27] R. Jin and G. Weng, "Active contours driven by adaptive functions and fuzzy c-means energy for fast image segmentation," *Signal Processing*, vol. 163, pp. 1–10, 2019, https://doi.org/10.1016/j.sigpro.2019.05.002.
[28] F. Pierre *et al.*, "Segmentation with Active Contours To cite this version : HAL Id : hal-03235096 Segmentation with Active Contours Introduction," *Image Processing On Line*, vol. 11, pp. 120-141, 2021, https://doi.org/10.5201/ipol.2021.298.
[29] U. Iruansi, "Power-line Insulator Defect Detection and Classification," *Doctoral dissertation*, 2018, https://researchspace.ukzn.ac.za/handle/10413/16858.
[30] S. Sanjaya, U. Adzkia, L. Handayani, and F. Yanto, "Local Binary Pattern and Learning Vector Quantization for Classification of Principal Line of Palm-Hand," *Indonesian Journal of Artificial Intelligence and Data Mining (IJAIDM)*, vol. 3, no. 2, pp. 71–77, 2020, https://ejournal.uin-suska.ac.id/index.php/IJAIDM/article/view/10236.
[31] A. D. Saputra, B. Irawan, and R. A. Nugrahaeni, "Detection of Skin Cancer M Elanom a Using Expert System Forw Ard Chaining M Ethod and Im Age Processing of K-Nearest Neighbor (Knn) M Ethod Based on Android," *Jurnal Sistem Cerdas*, vol. 1, no. 2, pp. 27–36, 2018, https://journal.binus.ac.id/index.php/SEEIJ/article/view/5561.
[32] P. Banerjee, A. K. Bhunia, A. Bhattacharyya, P. P. Roy, and S. Murala, "Local Neighborhood Intensity Pattern–A new texture feature descriptor for image retrieval," *Expert Syst Appl*, vol. 113, pp. 100–115, 2018, https://doi.org/10.1016/j.eswa.2018.06.044.
[33] A. Chahi, Y. Ruichek, and R. Touahni, "Local directional ternary pattern: A new texture descriptor for texture classification. Computer vision and image understanding," *Computer Vision and Image Understanding*, vol. 169, pp. 14-27, https://doi.org/10.1016/j.cviu.2018.01.004.
[34] N. K. Caecar Pratiwi, R. Magdalena, Y. N. Fuadah, and S. Saidah, "K-Nearest Neighbor for colon cancer identification," *J Phys Conf Ser*, vol. 1367, no. 1, 2019, https://doi.org/10.1088/1742-6596/1367/1/012023.
[35] N. Ali, D. Neagu, and P. Trundle, "Evaluation of k-nearest neighbour classifier performance for heterogeneous data sets," *SN Appl Sci*, vol. 1, no. 12, pp. 1–15, 2019, https://doi.org/10.1007/s42452-019-1356-9.
[36] A. Panda, R. B. Pachori, and N. D. Sinnappah-Kang, "Classification of chronic myeloid leukemia neutrophils by hyperspectral imaging using Euclidean and Mahalanobis distances," *Biomed Signal Process Control*, vol. 70, July 2021, https://doi.org/10.1016/j.bspc.2021.103025.
[37] V. Ramnarain-Seetohul, V. Bassoo, and Y. Rosunally, "Similarity measures in automated essay scoring systems:

A ten-year review," *Education and Information Technologies*, vol. 27, pp. 5573–5604, https://doi.org/10.1007/s10639-021-10838-z.
[38] O. E. Oduntan, I. A. Adeyanju, A. S. Falohun, and O. O. Obe, "A comparative analysis of euclidean distance and cosine similarity measure for automated essay-type grading," *Journal of Engineering and Applied Sciences*, vol. 13, no. 11, pp. 4198–4204, 2018, https://medwelljournals.com/abstract/?doi=jeasci.2018.4198.4204.
[39] K. Ghasvarian Jahromi, D. Gharavian, and H. Mahdiani, "A novel method for day-ahead solar power prediction based on hidden Markov model and cosine similarity," *Soft computing*, vol. 24, no. 7, pp. 4991-5004, 2020, https://doi.org/10.1007/s00500-019-04249-z.
[40] S. Paul and P. Maji, "City block distance and rough-fuzzy clustering for identification of co-expressed microRNAs," *Mol Biosyst*, vol. 10, no. 6, pp. 1509–1523, 2014, https://doi.org/10.1039/C4MB00101J.

BIOGRAPHY OF AUTHORS

Hilman Fauzi is a lecturer in the School of Electrical Engineering at Telkom University. He received a Master's degree in biomedical engineering from Institut Teknologi Bandung, Bandung, Indonesia, in 2013. Meanwhile, He received a Ph.D. degree from Universiti Teknologi Malaysia, Malaysia, and Indonesia in 2020. His research is on the electroencephalogram application in neural marketing and brain disorder, biomedical instrumentation, and medical image processing. Email: hilmanfauzitsp@telkomuniversity.ac.id

Cynthia Erika Magdalena received a Bachelor's degree in telecommunication engineering in 2021. His research interests include biomedical signal processing and telecommunication transmission. Email: cynthiaerikaa@student.telkomuniversity.ac.id

Sofia Sa'adiah is a lecturer in telecommunication engineering at Telkom University. She received her bachelor's and master's degree at Telkom University. Her research interests are image and audio processing, machine learning, deep learning, biomedical signal processing, and also watermarking. Email: sofiasaidahsfi@telkomuniversity.ac.id

Fahmi Oscandar is a lecturer in the Faculty of Dentistry, Universitas Padjadjaran Indonesia. He received his master's degree in Biology Oral from Universitas Padjadjaran in 2007. He finished his Ph.D. Program in Craniofacial Imaging Sub Forensic-Radiology of Universiti Sains Malaysia in 2017. His research is focused on odontology forensic radiology. Email: fahmi.oscandar@fkg.unpad.ac.id